Title: Low generation asymmetric dendrimers exhibit minimal toxicity and effectively complex DNA

Running Title: Asymmetric dendrimers for gene delivery

Neha Shah[1,2], Raymond J. Steptoe[2*], Harendra S. Parekh[1*].

[1]School of Pharmacy, The University of Queensland, Brisbane, QLD 4102, Australia and [2]The University of Queensland Diamantina Institute, Princess Alexandra Hospital, Woolloongabba, QLD 4102, Australia.

[*]These authors contributed equally.

Address correspondence to

Dr. Harendra S. Parekh,
School of Pharmacy,
The University of Queensland,
Brisbane, QLD 4102, Australia,
Tel: +61-7-3346 1887; Fax: +61-7-3346 1999
Email: h.parekh@uq.edu.au

Or

Dr. Raymond J. Steptoe,
The University of Queensland Diamantina Institute,
Princess Alexandra Hospital,
Level 4, R Wing, Building 1,
Woolloongabba, QLD 4102,
Australia
Tel: +61-7-3176 5395; Fax: +61-7-3176 5946
Email: r.steptoe@uq.edu.au

Abstract

Conventional dendrimers are spherical symmetrically branched polymers ending with active surface functional groups. Polyamidoamine (PAMAM) dendrimers have been widely studied as gene delivery vectors and have proven effective at delivering DNA to cells *in vitro*. However, higher generation (G4-G8) PAMAM dendrimers exhibit toxicity due to their high cationic charge density and this has limited their application *in vitro* and *in vivo*. Another limitation arises when attempts are made to functionalize spherical dendrimers as targeting moieties cannot be site-specifically attached. Therefore, we propose that lower generation asymmetric dendrimers, which are likely devoid of toxicity and to which site-specific attachment of targeting ligands can be achieved, would be a viable alternative to currently-available dendrimers. We synthesized and characterized a series of peptide-based asymmetric dendrimers and compared their toxicity profile and ability to condense DNA to spherical PAMAM G1 dendrimers. We show that asymmetric dendrimers are minimally toxic and condense DNA into stable toroids which have been reported necessary for efficient cell transfection. This paves the way for these systems to be conjugated with targeting ligands for gene delivery *in vitro* and *in vivo*.

Key words: asymmetric dendrimers; toroids; low-generation peptides; cytotoxicity and PAMAM G1.

Introduction

Dendrimers such as polyamidoamine (PAMAM) [1], polyethyleneimine (PEI) [2] and poly(L-lysine) (PLL) [3] have been used to facilitate delivery and expression of DNA [4], delivery of drugs and radiotherapeutics [5,6] and for *in vitro* and *in vivo* diagnostics [7]. Dendrimers are synthesized by either divergent [8] or convergent [9] approaches, each of which can give rise to linear or branched architectures, thus enabling the size and generation of the dendrimer to be controlled during synthesis. Commercially-available dendrimers such as PAMAM and PEI are formed in solution by sequentially coupling 'layers' of repeating branched monomer units starting from a central core and ending with NH_2, OH, CHO, COOMe, Boc, COONa or CH_3 termini, the NH_2 typically being employed in gene delivery. The surface amine groups of PAMAM and other dendrimers interact with negatively charged molecules (e.g. DNA, oligonucleotide, siRNA) allowing dendrimers to protect and transport these molecules to a wide variety of cell types (reviewed in [10]).

Of spherical dendrimers, PAMAM is the most widely used for *in vitro* gene delivery, with the primary focus being on the use of highly-branched ('high generation' G4 – G8) dendrimers which are predicted to possess between 64 and 1024 surface amine termini [1,11,12]. High generation PAMAM dendrimers have been found to facilitate more efficient transfection than the lower generation dendrimers. For example, *in vitro* studies performed using PAMAM G6 dendrimers showed maximal transfection whereas use of G10 dendrimers provided no significant increase in transfection efficiency [13] and PAMAM G2 dendrimers facilitate negligible plasmid DNA transfection relative to G4, G7 and G9 dendrimers [14]. PAMAM dendrimers modified with PEG or cyclodextrins have also been used to successfully achieve high transfection efficiency *in vitro* (reviewed in [15]).

Despite these results a major shortcoming of PAMAM dendrimers, that limits their use both *in vitro* and *in vivo* has been undesirable toxicity associated with their high surface cationic charge density and the excess positive charge associated with the high Nitrogen (dendrimer):Phosphate (DNA) ratios commonly employed [11,12]. For PAMAM dendrimers *in vitro,* toxicity has been shown to be generation-dependent with the G5 and G7 higher generation dendrimers exhibiting increasing cytotoxicity over G3 dendrimers [11] and higher-generation (≥ G4) PAMAM dendrimers are approximately three-fold more cytotoxic than G2 or G3 dendrimers [1]. Surface PEGylation of spherical dendrimers has been attempted to circumvent toxicity however, this has led to a reduced number of surface sites available for drug/gene conjugation/complexation [16,17]. For targeted delivery of DNA, another limitation of spherical PAMAM dendrimers is that there is a surplus of available reactive sites due to the stochastic synthesis. Therefore it is not possible to attach targeting ligands in a site-specific manner or distal to the DNA-complexing sites. Furthermore, PAMAM dendrimers are relatively expensive to manufacture, primarily due to the significant excess of monomer units required for traditional growth schemes, and the reduced purity of the desired end product obtained relative to solid phase synthesis [18].

One approach to overcoming the limitations of spherical dendrimers would be development of low-generation, asymmetric dendrimers that could be prepared on an insoluble solid-support, for example, by a technique commonly referred to as solid phase peptide synthesis (SPPS) [19-21]. One advantage of SPPS is that low-generation asymmetric dendrimers can be synthesized rapidly, in high purity and yield [20,22]. We propose the low cationic charge of such dendrimers, even at high N:P ratios, would not predispose them to the cytotoxicity observed with higher generation spherical dendrimers. By utilizing the well-established technique of SPPS, asymmetric dendrimers could be readily constructed to incorporate a well defined site for a

targeting-ligand, using an orthogonal protecting strategy where a targeting-ligand is site-specifically conjugated on a side-chain of the dendrimer distal to the DNA binding site [23]. Targeting moieties could be as diverse as antibodies [24], peptides and carbohydrates [25], (reviewed in [26]) depending on the target-cell of interest.

Here we describe an approach, using SPPS, for rapid synthesis of peptide-based low-generation asymmetric dendrimers. The physico-chemical characteristics of dendrimer-DNA binding, toxicity profile and morphology were compared for dendrimer/DNA complexes formed using either peptide-based asymmetric dendrimers or a commercially-available PAMAM G1 dendrimer, for comparison.

Materials and Methods

Materials

All fluorenylmethyloxycarbonyl (Fmoc) amino acids and Rink amide resin (200-400 mesh) were purchased from NovaBiochem (Australia) unless otherwise stated. The solvent employed throughout the synthesis was peptide grade *N*, *N*-Dimethylformamide (DMF; Merck) used without further purification. PAMAM G1, piperidine, trifluoroacetic acid (TFA) and ethidium bromide were purchased from Sigma-Aldrich. Dulbecco's modified Eagle's medium (DMEM) and Lipofectamine® were purchased from Invitrogen.

Instrumentation

Purification of asymmetric dendrimers was performed by reverse-phase high performance liquid chromatography (RP-HPLC). Preparative RP-HPLC was performed on a Waters HPLC system (Model 600 controller, 2996 photodiode array detector) with a C_4 column (Vydac, 5 μm pore size, id = 4.6 mm, 250 mm). Dendrimers were injected (~100 mg/batch) using a flow rate of 10 ml/min, isocratic conditions (100 % A) and purified with the mobile phase comprising solvent A (100 % H_2O), solvent B (90 % $CH_3CN_{(aq)}$).

Analytical RP-HPLC was performed using a Shimadzu HPLC system (controller- CBM-20A, pump A - LC-10AD, autosampler – SIL-10AXL, detector – SPD-10A) with a C_4 column and mobile phase comprised solvent A (0.02 % $HFBA_{(aq)}$) [27] and solvent B (90 % $CH_3CN_{(aq)}$). Analysis of each purified asymmetric dendrimer was undertaken at a flow rate of 1 ml/min, using the following conditions: 100 % A (0-20 min), then to 100 % B linearly over 10 min.

Liquid chromatography/mass spectrometry (LC-MS) was performed using an Applied Biosystems/MDS Sciex Q-TRAP LC/MS/MS system. For ESI^+-MS, each asymmetric dendrimer was dissolved in 50 % $CH_3CN_{(aq)}$ to 300 μg/ml and observed for the molecular ion.

NMR spectroscopy was performed using a Bruker Topsin 400/500 NMR spectrometer (400/500MHz). Each asymmetric dendrimer was dissolved in D_2O with one or two drops of dioxane as an internal reference for ^{13}C NMR and dendrimer assignments confirmed with the aid of 1D and 2D NMR.

Asymmetric dendrimer synthesis

Asymmetric dendrimers were synthesized as previously described [28], on a 0.5 mmol scale using Fmoc SPPS [20,29]. Rink amide resin (0.6 mmol/g loading capacity) was swollen in DMF in a sintered glass vessel for 60 min followed by Fmoc deprotection with 20 % *v/v* piperidine in DMF (2 × 8 min washes). All amino acids were pre-activated prior to coupling using *O*-benzotriazole-*N, N, N', N'*-tetramethyl-uronium-hexafluoro-phosphate (HBTU; 0.5 M in DMF) and *N*, *N*-diisopropylethylamine (DIPEA). Each coupling step was monitored for ninhydrin values of ≥ 99 % using a quantitative colour test devised to detect the presence of free amino groups spectrophotometrically [30], the Fmoc group was then deprotected as outlined above. The Rink amide resin was treated with Fmoc-protected amino acids (except for arginine which is both Fmoc and Pbf protected) in the following sequence:

4^+ Arginine (Figure. 1-2): Glycine (Gly) (3 equiv), Gly (2 equiv), Gly (2 equiv), Lysine (Lys) (2 equiv), Arginine (Arg) (5 equiv). Terminal Fmoc protected groups were deprotected using 20 % *v/v* piperidine in DMF, the resin was then washed with DCM and dried *in vacuo.* The Pbf protecting group was removed during acidolytic cleavage of the dendrimers off-resin using

TFA:DCM:H_2O:TIPS (90:5:2.5:2.5; 3 h). The mixture was filtered and TFA removed *in vacuo*. The mixture was then co-evaporated with toluene (3 × 15 ml), and triturated with ice cold diethyl ether. The dendrimer (crude) was reconstituted in water and lyophilized. ^{1}H NMR (D_2O) δ (ppm): 1.30 – 1.85 (Rβ, R_1β, Kβ, Kδ , Rγ, R_1γ, Kγ, C$\underline{H}_2$, 14H, m), 3.09 – 3.17 (Rδ, R_1δ, Kδ, C$\underline{H}_2$, 6H, m), 3.76 – 3.93 (Rα, C$\underline{H}$, $G_{1\text{-}2}$α, Gα, C$\underline{H}_2$, 7H, m), 3.96 – 3.99 (R_1α, C$\underline{H}$, 1H, t, J = 6.61 Hz), 4.21 – 4.24 (Kα, C$\underline{H}$, 1H, t, J = 7.43 Hz). ^{13}C NMR (D_2O) δ (ppm): 23.59 (Kγ, $\underline{C}H_2$), 24.56 (R_1γ, $\underline{C}H_2$), 24.81 (Rγ, $\underline{C}H_2$), 29.8 (Kδ, $\underline{C}H_2$), 29.18 (R_1β, $\underline{C}H_2$), 29.27 (Rβ, $\underline{C}H_2$), 31.56 (Kβ, $\underline{C}H_2$), 40.46 (R_1δ, $\underline{C}H_2$), 41.50 (Rδ, $\underline{C}H_2$), 41.61 (Kε, $\underline{C}H_2$), 43.19 (Gα, $\underline{C}H_2$), 43.58 (G_1α, $\underline{C}H_2$), 43.65 (G_2α, $\underline{C}H_2$), 53.71 (R_1α, $\underline{C}$H), 54.14 (Rα, $\underline{C}$H), 55.45 (Kα, $\underline{C}$H), 158.01 (R2, $R_1$2, $\underline{C}$=NH), 170.45 - 170.91 (R, R_1, $\underline{C}$=O), 173.10 ($G_{1\text{-}2}$, G, $\underline{C}$=O), 175.49 (K, $\underline{C}$=O). Yield: 0.065 g (65 %). ESI$^+$-MS *m/z*: ($C_{24}H_{48}N_{14}O_6$) calculated 628.39, found 629.50 $[M + H]^+$. R_t: 11.35 min.

8$^+$ *Arginine* (Figure. 1-3): Gly (3 equiv), Gly (2 equiv), Gly (2 equiv), Lys (2 equiv), Lys (3 equiv), Arg (6 equiv). The same process was followed as outlined for 4$^+$ Arginine above. ^{1}H NMR (D_2O) δ (ppm): 1.23 – 1.83 (Kγ, $K_{1\text{-}2}$γ, Kδ, $K_{1\text{-}2}$δ, Rγ, $R_{1\text{-}3}$γ, Kβ, $K_{1\text{-}2}$β, Rβ, $R_{1\text{-}3}$β, C$\underline{H}_2$, 34H, m), 3.06 – 3.13 (Kε, $K_{1\text{-}2}$ε, Rδ, $R_{1\text{-}3}$δ, C$\underline{H}_2$, 14H, m), 3.82 (Gα, C$\underline{H}_2$, 2H, s), 3.90 ($G_{1\text{-}2}$α, C$\underline{H}_2$, $R_{1\text{-}3}$α, C$\underline{H}$, 6H, s), 3.95 – 4.00 (Rα, C$\underline{H}$, 2H, m), 4.11 – 4.22 ($K_{1\text{-}2}$α, Kα, C$\underline{H}$, 3H, t, J = 7.30 Hz). ^{13}C NMR (D_2O) δ (ppm): 23.62 - 23.75 (Kγ, $K_{1\text{-}2}$γ, $\underline{C}H_2$), 24.65 - 24.81 (Rγ, $R_{1\text{-}3}$γ, $\underline{C}H_2$), 28.98 - 29.26 (Rβ, $R_{1\text{-}3}$β, Kδ, $K_{1\text{-}2}$δ, $\underline{C}H_2$), 31.67 - 31.74 (Kβ, $K_{1\text{-}2}$β, $\underline{C}H_2$), 40.29 - 40.50 (Rδ, $R_{1\text{-}3}$δ, $\underline{C}H_2$), 41.49 - 41.62 (Kε, $K_{1\text{-}2}$ε, $\underline{C}H_2$), 43.23 - 43.72 (Gα, $G_{1\text{-}2}$α, $\underline{C}H_2$), 53.71 ($R_{1\&3}$α, $\underline{C}$H), 54.14 (Rα, R_2α, $\underline{C}$H), 55.10 (K_2α, $\underline{C}$H), 55.28 (K_1α, $\underline{C}$H), 55.67 (Kα, $\underline{C}$H), 158.01 (R, $R_{1\text{-}3}$2, $\underline{C}$=NH), 170.45 - 170.77 (R, $R_{1\text{-}2}$, $\underline{C}$=O), 173.17 - 173.19 (G, $G_{1\text{-}2}$, $\underline{C}$=O), 174.57 (K_2, $\underline{C}$=O), 174.91 (R_3, $\underline{C}$=O), 175.33 (K, $\underline{C}$=O), 175.75 (K_1, $\underline{C}$=O). Yield: 0.063 g (63 %). ESI$^+$-MS *m/z*: ($C_{48}H_{96}N_{26}O_{10}$) calculated 1197.44, found 1198.00 $[M + H]^+$. R_t: 13.28 min.

4^{+} *Lysine* (Figure. 1-4): Gly (3 equiv), Gly (2 equiv), Gly (2 equiv), Lys (2 equiv), Lys (3 equiv). The same process was followed as outlined for 4^{+} Arginine above. ^{1}H NMR (D_2O) δ (ppm): 1.21 – 1.85 (Kγ, $K_{1\text{-}2}$γ, Kδ, $K_{1\text{-}2}$δ, Kβ, $K_{1\text{-}2}$β, C$\underline{H}_2$, 18H, m), 2.86 – 2.89 ($K_{1\text{-}2}$ε, C$\underline{H}_2$, 4H, m), 3.10 – 3.13 (Kε, C$\underline{H}_2$, 2H, t, *J* = 7.18 Hz), 3.77 – 3.93 ($K_{1\text{-}2}$α, C$\underline{H}$, Gα, $G_{1\text{-}2}$α, C$\underline{H}_2$, 8H, m), 4.21 – 4.24 (Kα, C$\underline{H}$, 1H, t, *J* = 7.18 Hz). ^{13}C NMR (D_2O) δ (ppm): 22.25 (K_1γ, $\underline{C}H_2$), 22.56 (K_2γ, $\underline{C}H_2$), 23.58 (Kγ, $\underline{C}H_2$), 27.60 (K_1δ, K_2δ, $\underline{C}H_2$), 29.11 (Kδ, $\underline{C}H_2$), 31.60 ($K_{1\text{-}2}$β, $\underline{C}H_2$), 31.65 (Kβ, $\underline{C}H_2$), 40.20 ($K_{1\text{-}2}$ε, $\underline{C}H_2$), 40.48 (Kε, $\underline{C}H_2$), 43.18 (Gα, $\underline{C}H_2$), 43.56 (G_1α, $\underline{C}H_2$), 43.65 (G_2α, $\underline{C}H_2$), 53.93 (K_2α, $\underline{C}H_2$), 54.35 (K_1α, $\underline{C}H$), 55.39 (Kα, $\underline{C}H$), 170.55 – 170.95 ($K_{1\text{-}2}$, $\underline{C}$=O), 173.06 – 173.14 (G, $G_{1\text{-}2}$, $\underline{C}$=O), 175.33 – 175.40 (K, $\underline{C}$=O). Yield: 0.083 g (83 %). ESI^{+}-MS *m/z*: ($C_{24}H_{48}N_{10}O_6$) calculated 572.70, found 573.50 $[M + H]^{+}$. R_t: 10.29 min.

8^{+} *Lysine* (Figure. 1-5): Gly (3 equiv), Gly (2 equiv), Gly (2 equiv), Lys (2 equiv), Lys (3 equiv), Lys (5 equiv). The same process was followed as outlined for 4^{+} Arginine above. ^{1}H NMR (D_2O) δ (ppm): 1.25 – 1.79 (Kγ, $K_{1\text{-}6}$γ, Kδ, $K_{1\text{-}6}$δ, Kβ, $K_{1\text{-}6}$β, C$\underline{H}_2$, 42H, m), 2.86 – 2.91 ($K_{1\text{-}6}$ε, C$\underline{H}_2$, 12H, q), 3.08 – 3.11 (Kε, C$\underline{H}_2$, 2H, m), 3.81 – 3.91 ($K_{3\text{-}6}$α, C$\underline{H}$, Gα, G_1α, G_2α, C$\underline{H}_2$, 10H, m), 4.11 (K_2α, C$\underline{H}$, 1H, t, *J* = 7.01 Hz), 4.15 (K_1α, C$\underline{H}$, 1H, t, *J* = 7.01 Hz), 4.22 (Kα, C$\underline{H}$, 1H, t, *J* = 7.25 Hz). ^{13}C NMR (D_2O) δ (ppm): 22.38 - 22.57 ($K_{1\text{-}6}$γ, $\underline{C}H_2$), 23.67 - 23.76 (Kγ, $\underline{C}H_2$), 27.56 - 27.59 ($K_{1\text{-}6}$δ, $\underline{C}H_2$), 29.16 - 29.22 (Kδ, $\underline{C}H_2$), 31.60 - 31.98 (Kβ, $K_{1\text{-}6}$β, $\underline{C}H_2$), 40.20 - 40.54 (Kε, $K_{1\text{-}6}$ε, $\underline{C}H_2$), 43.21 - 43.70 (Gα, $G_{1\text{-}2}$α, $\underline{C}H_2$), 53.95 ($K_{4\&6}$α, $\underline{C}$H), 54.36 ($K_{3\&5}$α, $\underline{C}$H), 54.98 (Kα, $\underline{C}$H), 55.36 (K_1α, $\underline{C}$H), 55.51(K_2α, $\underline{C}$H), 170.53 - 170.82 (K_1, $\underline{C}$=O), 173.11 (G, $G_{1\text{-}2}$, $\underline{C}$=O), 174.40 (K_2, $\underline{C}$=O), 174.81 (K, $\underline{C}$=O), 175.29 ($K_{3\&5}$, $\underline{C}$=O), 175.70 ($K_{4\&6}$, $\underline{C}$=O). Yield: 0.062 g (62 %). ESI^{+}-MS *m/z*: ($C_{48}H_{96}N_{18}O_{10}$) calculated 1085.39, found 1086.00 $[M + H]^{+}$. R_t: 13.10 min.

Plasmid preparation

E .coli were transformed with a 4.3 kb plasmid (pEGFP-C1) encoding green fluorescent protein under control of a CMV promoter and grown in Luria broth (37°C, 16 h) on a shaker at 300 rpm. Plasmid DNA was recovered using an endotoxin-free megaprep kit (Qiagen). DNA concentration was determined by UV absorbance at 260 and 280 nm after redissolving in water.

Ethidium bromide assay

DNA (pEGFP-C1, 0.2 μg) was mixed with dendrimer (1 mg/ml) at various N:P ratios in distilled water and incubated for 30 min at room temperature. After 30 min, ethidium bromide (EtBr) added at an EtBr:DNA base pair ratio of 1:4 [31]. Fluorescence was measured (either 485 nm Ex, 590 nm Em or 544 nm Ex and 590 nm Em) using a FLUOstar Optima microplate reader (BMG Labtech Pty. Ltd., Victoria, Australia).

Transmission electron microscopy (TEM)

Dendrimer/DNA complexes were prepared as described above and, at defined times after mixing, stained as previously described [32]. Briefly, 400 mesh formvar-free carbon coated grids were glow discharged for 30 sec. A 5 μl drop of dendrimer/DNA complex solution was carefully placed on the grid and immediately stained with 1 % uranyl acetate and 15 – 30 sec later excess liquid was wicked off with filter paper. Grids were air-dried prior to viewing (JEM – 1010 JEOL, Tokyo, 100 kV), images were captured using a digital camera (SoftImaging® Megaview III) and analysed using SoftImaging®.

Cytotoxicity assay

Human embryonic kidney 293T cells were grown in culture medium (DMEM 10 % FCS) and seeded in a 24-well plate (3×10^6/well) in 500 μl of medium. Cells were incubated overnight (37°C, 5 % CO_2) to reach 50 – 60 % confluency. Dendrimer/DNA complexes were prepared as described above and after 30 min incubation the solution was made isotonic by addition of 1/10 volume of 10 × PBS. The medium was then replaced by 500 μl of fresh culture medium and isotonic dendrimer solution. After a further 4 h, the dendrimer/DNA solution was replaced with fresh culture medium and cells cultured for a further 24 h. Lipofectamine® transfection was performed according to manufacturer's instructions and cultured for 24 h total. Non-adherent cells were harvested and pooled with adherent cells recovered by trypsinisation. Viability was assessed by flow cytometry (BD FACScalibur™) after staining with propidium iodide.

Results

Synthesis and characterization of asymmetric dendrimers

Asymmetric dendrimers with 4 or 8 terminal amines constructed with either arginine ('4^+ Arginine', '8^+ Arginine') or lysine ('4^+ Lysine', '8^+ Lysine') terminal amino acids (Figure. 1-2 - 1-5) were synthesized using Fmoc SPPS. After purification using preparative RP-HPLC, all dendrimers were obtained in good yield (60 – 85 %). The molecular weight of each dendrimer was confirmed by ESI^+-MS where the molecular ion of the dendrimer was identified. Both 1D and 2D NMR spectroscopy (^1H and ^{13}C) were used for definitive assignments, although given the complexity of spectra for the arginine dendrimers in particular; ^1H and ^{13}C NMR of L-arginine alone were also undertaken. The data confirmed successful synthesis of the panel of asymmetric dendrimers (Figure. 1-2 - 1-5 and supporting information).

Assessment of DNA complexation using ethidium bromide fluorescence

Ethidium bromide dye fluoresces when intercalated with DNA. As EtBr is prevented from intercalating with DNA in the presence of a complexing polycation, loss of fluorescence is a convenient measure of polycation/DNA complexation. Based on loss of fluorescence, PAMAM G1 effectively complexed DNA at N:P ratios $\geq$ 0.5:1 (Figure. 2A). Of the four asymmetric dendrimers, 8^+ Arginine and 4^+ Arginine complexed DNA with the most reproducible results and at N:P ratios as low as 5:1 (Figure. 2B and 2D). 8^+ Lysine complexed DNA less reproducibly and at N:P ratios $\geq$ 5:1, whereas 4^+ Lysine least reproducibly complexed DNA (Figure. 2C and 2E). Overall, asymmetric dendrimers constructed with arginine as the terminal amino acid complexed DNA more reproducibly, and at lower N:P ratios than those with lysine as the terminal amino acid.

Asymmetric dendrimers form toroidal complexes with DNA

Transmission electron microscopy (TEM) was used to characterize the morphology of dendrimer/DNA complexes. Our aim was to investigate whether toroidal structures were formed as these have been reported as characteristic of DNA complexation in other polycationic systems [33,34]. For these studies we chose to compare 8^+ Arginine, which possessed the best DNA complexing characteristics in the EtBr assay, with PAMAM G1. At a 1:1 N:P ratio of PAMAM G1 to DNA, we observed a meshwork of pleiomorphic structures (Figure. 3A). As the N:P ratio was increased to 5:1, individual rod and toroid-like structures, which often formed small clusters of two to three rods or toroids, were observed (Figure. 3B). At a 10:1 N:P ratio, individual toroids, which rarely formed clusters, were observed (Figure. 3C) and structures that resembled elongated or distorted toroids were frequently present, whilst rod-like structures were rarely observed. Of the PAMAM G1/DNA complexes formed at a 10:1 N:P ratio approximately 40 % were individual toroids ranging between 35 and 110 nm and had a mean diameter of 61 ± 14 nm (mean ± SD). We next determined the morphology of dendrimer/DNA complexes formed by 8^+ Arginine. At a 1:1 N:P ratio, an extensive netted or meshwork structure was observed (Figure. 3D) similar to that seen with PAMAM G1 at this ratio (Figure. 3A). At a 5:1 N:P ratio elongated and segmented structures were observed (Figure. 3E), whereas at 10:1 toroid-like structures, present almost exclusively in clusters, were observed (Figure. 3F). Of 8^+ Arginine/DNA complexes formed at a 10:1 N:P ratio, approximately 46 % comprised clusters of toroids and 15 % comprised individual toroids with a mean diameter 67 ± 17 nm (mean ± SD). For both PAMAM G1 and 8^+ Arginine, observed complexes not exhibiting a toroidal appearance were either elongated and distorted toroids or pleiomorphic in shape.

To better understand the behaviour and stability of dendrimer/DNA complexes, a time-course study was performed comparing PAMAM G1 and 8^+ Arginine where morphology was observed 10, 20, 30, 45, 60 and 120 min after addition of DNA to dendrimers at a 10:1 N:P ratio. Between 10 and 30 min, PAMAM G1/DNA comprised primarily toroids with few rods (see Table 1). The proportion of rods then increased and outnumbered toroids at 60 and 120 min (see Table 1). For 8^+ Arginine/DNA at a 10:1 N:P ratio, we observed clusters of toroids and this changed little over time, however, toroids appeared most numerous between 20 and 30 min after DNA/dendrimer mixing (see Table 2). Overall, both PAMAM G1/DNA and 8^+ Arginine/DNA formed 'toroidal' structures at all time points tested. However, 8^+ Arginine/DNA showed a disposition to form clusters of toroids whereas PAMAM G1/DNA formed individual toroids. Based on the time-course study, complexes between DNA and asymmetric dendrimers formed toroids that were stable over the time period tested.

Asymmetric dendrimers effectively complex DNA in physiological salt solutions

For effective gene transfer *in vitro* or *in vivo*, dendrimer/DNA complexes must be stable in physiological salt solutions. Therefore, we next established whether ions present in phosphate buffer (PB) or sodium chloride-containing phosphate buffered saline (PBS) could interfere with dendrimer/DNA complexation. To this end, the EtBr assay was used to compare complexation of DNA by dendrimers in saline, PB and PBS. When complexed in saline and PB, PAMAM G1 inhibited EtBr fluorescence indicating complex formation whereas complexes formed in PBS inhibited EtBr fluorescence only when a high N:P ratio of 50:1 was used (Figure. 4A). Similarly, 8^+ Arginine effectively complexed DNA in water, saline and PB as indicated by the EtBr assay (Figure. 4B). Likewise, for 8^+ Arginine in PBS, EtBr fluorescence was inhibited when a high N:P ratio of 100:1 was tested signifying efficient complexation. This data suggests

that counter-ions present within the solvent influence DNA complexation by asymmetric dendrimers and that the presence of the ions in PBS hinders effective complexation at low N:P ratios.

Asymmetric dendrimer/DNA complexes exhibit minimal cytotoxicity

To establish the cytotoxicity profile, DNA complexed with PAMAM, asymmetric dendrimers or Lipofectamine® were incubated with HEK 293T cells for 4 h and cell viability was tested using a FACS-based propidium iodide assay a further 20 h later. PAMAM G1/DNA complexes exhibited minimal toxicity to HEK 293T cells at all N:P ratios tested up to 100:1 (Figure. 5). This was in distinct contrast to Lipofectamine®, which killed approximately 40 % of cells under the same conditions. A higher generation PAMAM dendrimer (G4) was also tested at an N:P ratio of 10:1 and this resulted in approximately 20 % cell death which increased to approximately 60 % when the N:P ratio was increased to 100:1(data not shown). In contrast, 8^{+} Arginine/DNA at all N:P ratios tested ($\leq$ 100:1 N:P ratio) showed low cytotoxicity with cell viabilities in the range of 90 – 98 % observed (Figure. 5). The data suggests that even at high N:P ratios required for complete complexation of DNA, low generation asymmetric peptide dendrimers display negligible cytotoxicity.

Discussion

In vivo use of commercially-available high-generation (G4-G10) PAMAM and other spherical dendrimers is limited by cytotoxicity due to their high cationic charge density, while attempts to functionalize these systems with targeting moieties unavoidably generates heterogeneous end-products. We propose that low-generation asymmetric dendrimers, which are devoid of cytotoxicity and that permit site-specific attachment of a targeting ligand, distal to the site of DNA complexation would be a viable alternative to currently-available symmetrical dendrimers. We report the synthesis and characterisation of novel asymmetric low-generation dendrimers that effectively complex DNA and exhibit low cytotoxicity, even when complexed with DNA at high N:P ratios.

Fmoc-based SPPS, a relatively simple and cost-effective synthesis method was used to construct the asymmetric dendrimers and post-synthesis analysis by ESI^+-MS and NMR spectra confirmed that the dendrimers synthesized corresponded to the intended structures shown in Figure. 1 (1-2 – 1-5). We conclude that the results of the EtBr assay and TEM imaging indicate that, dependent on the number and nature of terminal amines, low-generation asymmetric dendrimers can effectively complex plasmid DNA with 8^+ Arginine in particular, most efficiently complexing DNA.

The TEM study performed here showed the presence of clusters of toroids formed by 8^+ Arginine/DNA. This is consistent with previous demonstrations that toroids form upon polycation and DNA complexation [32,35-39] and these generally range from approximately 40 to 90 nm in diameter [36,37,40]. We selected a wider range (35 to 110 nm) here to ensure all toroids that fell in the 40 – 90 nm ranges were included for quantitation. In TEM images of 8^+

Arginine/DNA complexes, toroids existed primarily in clusters whereas PAMAM G1 formed primarily 'non-clustering' toroids. Differences in the propensity to form 'clustering' toroids could be attributable to the marked differences in the physico-chemical properties of asymmetric and spherical dendrimers. For example, asymmetric dendrimers, due to the potentially-fixed stereochemistry of amide bonds formed between the constituent amino acids and the 'polarised' nature of the molecule with terminal amines concentrated in the 'head' region, may permit more interaction between the 'tails' than is possible for spherical dendrimers which exhibit a more uniform arrangement of terminal amines. Although there are reports of PAMAM G1 complexing DNA this has been seen only when PAMAM G1 is used in conjunction with lipid or other cationic helper molecules [41-43]. To our knowledge, this is the first detailed report demonstrating formation of toroidal dendrimer/DNA complexes by PAMAM G1 in the absence of helper molecules. The subtle irregularities in the size and shape of the toroids and rods we observed for dendrimer/DNA complexes are similar to those reported in the literature for other systems [37], and such variations in the morphology of dendrimer/DNA complexes appears normal. Based on our time-course studies, we found that there was little difference in the morphology of dendrimer/DNA complexes across the time-points tested. However, for PAMAM G1/DNA complexes a difference was noted in the proportion of rods to toroids which increased from 30 min after mixing of PAMAM and DNA. This suggests the optimal incubation time for PAMAM G1/DNA complexes beyond which their morphology reverts to rods is around 30 min. On the other hand, with increasing time there was little difference in the morphology of 8^{+} Arginine/DNA complexes suggesting an extended period of stability for these complexes, relative to PAMAM G1/DNA complexes.

For TEM, we tested 8^{+} Arginine/DNA at various N:P ratios (data not shown) but chose to work with an N:P ratio of 10:1 as at higher N:P ratios, the fixed concentration of DNA led to dendrimer/DNA complexes becoming more sparsely distributed on TEM grids. Additionally, we also found that increasing dendrimer concentration above 1 mg/ml resulted in large-scale aggregation. Although aggregation of dendrimer/DNA complexes has not been reported in TEM analysis, PAMAM dendrimers (≥ G1) have been shown to cause cell damage *in vitro* at concentrations greater than 1 mg/ml [12], and this may reflect findings similar to ours. Therefore, we conclude the optimal dendrimer concentration for forming complexes with DNA is 1 mg/ml for the asymmetric dendrimers tested here.

A hierarchy of complexing effectiveness was observed among the arginine and lysine series of asymmetric dendrimers, with the arginine series complexing DNA with apparently greater affinity than lysine. Others have reported similar or more efficient DNA complexation by arginine termini relative to lysine or other amino acids [44-46]. Arginine possesses a guanidinium moiety, which, with a pKa ≈ 13[47] is protonated over a wide pH range [48]. Guanidinium groups and DNA form characteristic pairs of parallel hydrogen bonds that provide binding strength by their charge and structural organization. These features are consistent with the demonstrated role for guanidinium groups in the arginine amino acid residues playing key roles in DNA-binding by proteins, such as histones. Furthermore, due to it's high pKa, arginine can also buffer the endosomal environment, a crucial factor in promoting release of DNA from endosomal compartment so transfection can take place [49]. Therefore, likely advantages of arginine-containing dendrimers are not only that DNA-binding should be relatively insensitive to pH variations during *in vitro* transfer and intracellular trafficking [48] but that they should also increase transfection efficiency.

We established that ions within the solvents used for asymmetric dendrimer/DNA complexation can adversely affect their formation. Although a slight effect of PB or NaCl solutions was observed this was minor. Interestingly, we noted that PBS, a reagent typically employed during *in vitro* studies inhibited dendrimer/DNA complexation at low N:P ratios. However, this would be unlikely to affect the use of asymmetric dendrimers where physiological salt solutions are required as we demonstrated that complexes formed at a high N:P ratio did not result in dissociation of dendrimer from DNA. Therefore, asymmetric dendrimers would be suitable for *in vitro* and *in vivo* use.

Our data demonstrates that both low-generation asymmetric dendrimer/DNA complexes and PAMAM G1/DNA complexes exhibit low cytotoxicity. These findings are consistent with a previous report in which PAMAM G1, but not higher generation (up to G4) PAMAM dendrimers exhibited little cytotoxicity *in vitro* [12]. Overall, and in general, specifically for asymmetric dendrimers, low generation dendrimers exhibit low cytotoxicity. An important safety advantage of asymmetric dendrimers described here is that, asymmetric dendrimers will be degraded to harmless natural amino acids, whereas PAMAM dendrimers, upon degradation, may form toxic methacrylates.

In conclusion, the studies described here demonstrate that peptidic asymmetric dendrimers can be constructed with ease, exhibit minimal cytotoxicity and effectively complex DNA. We propose that peptidic asymmetric dendrimer/DNA complexes engineered using SPPS are a new dendrimer family that, when suitably modified and targeted by a range of ligands, will be an effective system for efficient and safe DNA delivery *in vivo*.

Acknowledgements

We thank Dr. Tri Le for assisting with NMR assignments. We would also like to thank Dr. Matthias Floetenmeyer for providing carbon coated grids and Dr. Richard Webb for technical assistance with TEM imaging.

Supporting information

Supporting information may be found in the online version of this article.

Abbreviations

DNA – deoxyribonucleic acid, siRNA – short interfering ribonucleic acid, PEG – poly (ethylene glycol), H_2O – water, D_2O – deuterium oxide, CH_3CN – acetonitrile, HFBA – heptafluorobutyric acid, Fmoc – fluorenylmethoxycarbonyl, Pbf - 2,2,4,6,7-pentamethyldihydrobenzofuran-5-sulfonyl, DCM – dichloromethane, TIPS – triisopropyl silane, R_t – retention time , FCS – foetal calf serum, PBS – phosphate buffer saline.

References

1. Haensler, J.; Szoka Jr, F. C. *Bioconjugate Chemistry* 1993, **4**, 372-379.
2. Lungwitz, U.; Breunig, M.; Blunk, T.; Gopferich, A. *European Journal of Pharmaceutics and Biopharmaceutics* 2005, **60**, 247-266.
3. Ohsaki, M.; Okuda, T.; Wada, A.; Hirayama, T.; Niidome, T.; Aoyagi, H. *Bioconjugate Chemistry* 2002, **13**, 510-517.
4. Dufes, C.; Uchegbu, I. F.; Schatzlein, A. G. *Advanced Drug Delivery Reviews* 2005, **57**, 2177-2202.
5. Balogh, L. P.; Nigavekar, S. S.; Sung, L. Y.; Balogh, P.; Shi, X. Y.; Cook, A. T.; Minc, L. D.; Khan, M. K. *Journal of Nuclear Medicine* 2003, **44**, 1094.
6. Boas, U.; Heegaard, P. M. H. *Chemical Society Reviews* 2004, **33**, 43-63.
7. Herborn, C. U.; Barkhausen, J.; Paetsch, I.; Hunold, P.; Mahler, M.; Shamsi, K.; Nagel, E. *Radiology* 2003, **229**, 217-223.
8. Tomalia, D. A. *Macromolecular Symposia* 1996, **101**, 243-255.
9. Hawker, C. J.; Frechet, J. M. J. *Journal of the American Chemical Society* 1990, **112**, 7638-7647.
10. Eichman, J. D.; Bielinska, A. U.; Kukowska-Latallo, J. F.; Baker, J. R., Jr. *Pharm Sci Technol* 2000, **3**, 232-245.
11. Roberts, J. C.; Bhalgat, M. K.; Zera, R. T. *Journal of Biomedical Materials Research* 1996, **30**, 53-65.
12. Malik, N.; Wiwattanapatapee, R.; Klopsch, R.; Lorenz, K.; Frey, H.; Weener, J. W.; Meijer, E. W.; Paulus, W.; Duncan, R. *Journal of Controlled Release* 2000, **65**, 133-148.
13. KukowskaLatallo, J. F.; Bielinska, A. U.; Johnson, J.; Spindler, R.; Tomalia, D. A.; Baker, J. R. *Proceedings of the National Academy of Sciences of the United States of America* 1996, **93**, 4897-4902.
14. Braun, C. S.; Vetro, J. A.; Tomalia, D. A.; Koe, G. S.; Koe, J. G.; Middaugh, C. R. *Journal of Pharmaceutical Sciences* 2005, **94**, 423-436.
15. Svenson, S.; Tomalia, D. A. *Advanced Drug Delivery Reviews* 2005, **57**, 2106-2129.
16. Krishna, T. R.; Jain, S.; Tatu, U. S.; Jayaraman, N. *Tetrahedron* 2005, **61**, 4281-4288.
17. Boyd, B. J. *Expert Opinion on Drug Delivery* 2008, **5**, 69-85.
18. Merritt, A. T. *Combinatorial Chemistry & High Throughput Screening* 1998, **1**, 57-72.
19. Merrifield, R. B. *Journal of the American Chemical Society* 1963, **85**, 2149-2154.
20. Chan, W. C.; White, P. D.; Oxford University Press: New York, 2000, p 9 - 40 Chapter 42.
21. Atherton, E.; Sheppard, R. C.; IRL Press at Oxford University Press: Oxford, England; New York, 1989, p 13 - 37 Chapter 12 and pp 47 - 61 Chapter 15
22. Sheppard, R. *Journal of Peptide Science* 2003, **9**, 545-552.
23. Kumar, P.; Ban, H. S.; Kim, S. S.; Wu, H. Q.; Pearson, T.; Greiner, D. L.; Laouar, A.; Yao, J. H.; Haridas, V.; Habiro, K.; Yang, Y. G.; Jeong, J. H.; Lee, K. Y.; Kim, Y. H.; Kim, S. W.; Peipp, M.; Fey, G. H.; Manjunath, N.; Shultz, L. D.; Lee, S. K.; Shankar, P. *Cell* 2008, **134**, 577-586.
24. Roberts, J. C.; Adams, Y. E.; Tomalia, D.; Mercer-Smith, J. A.; Lavallee, D. K. *Bioconjugate Chem* 1990, **1**, 305-308.
25. Fajac, I.; Briand, P.; Monsigny, M. *Glycoconjugate Journal* 2001, **18**, 723-729.
26. Parekh, H. S. *Current Pharmaceutical Design* 2007, **13**, 2837-2850.

27. Mutalik, S.; Hewavitharana, A. K.; Shaw, P. N.; Anissimov, Y. G.; Roberts, M. S.; Parekh, H. S. *Journal of Chromatography B* 2009, **877**, 3556-3562.
28. Parekh, H. S.; Marano, R. J.; Rakoczy, E. P.; Blanchfield, J.; Toth, I. *Bioorganic & Medicinal Chemistry* 2006, **14**, 4775-4780.
29. URL.
30. Sarin, V. K.; Kent, S. B. H.; Tam, J. P.; Merrifield, R. B. *Analytical Biochemistry* 1981, **117**, 147-157.
31. Wiethoff, C. M.; Gill, M. L.; Koe, G. S.; Koe, J. G.; Middaugh, C. R. *Journal of Pharmaceutical Sciences* 2003, **92**, 1272-1285.
32. Bottcher, C.; Endisch, C.; Fuhrhop, J. H.; Catterall, C.; Eaton, M. *Journal of the American Chemical Society* 1998, **120**, 12-17.
33. Bloomfield, V. A. *Biopolymers* 1991, **31**, 1471-1481.
34. Arscott, P. G.; Ma, C. L.; Wenner, J. R.; Bloomfield, V. A. *Biopolymers* 1995, **36**, 345-364.
35. Slita, A. V.; Kasyanenko, N. A.; Nazarova, O. V.; Gavrilova, II; Eropkina, E. M.; Sirotkin, A. K.; Smirnova, T. D.; Kiselev, O. I.; Panarin, E. F. *Journal of Biotechnology* 2007, **127**, 679-693.
36. Dunlap, D. D.; Maggi, A.; Soria, M. R.; Monaco, L. *Nucleic Acids Research* 1997, **25**, 3095-3101.
37. Golan, R.; Pietrasanta, L. I.; Hsieh, W.; Hansma, H. G. *Biochemistry* 1999, **38**, 14069-14076.
38. Martin, A. L.; Davies, M. C.; Rackstraw, B. J.; Roberts, C. J.; Stolnik, S.; Tendler, S. J. B.; Williams, P. M. *Febs Letters* 2000, **480**, 106-112.
39. Bielinska, A. U.; KukowskaLatallo, J. F.; Baker, J. R. *Biochimica Et Biophysica Acta-Gene Structure and Expression* 1997, **1353**, 180-190.
40. Tang, M. X.; Li, W. J.; Szoka, F. C. *Journal of Gene Medicine* 2005, **7**, 334-342.
41. Takahashi, T.; Kono, K.; Itoh, T.; Emi, N.; Takagishi, T. *Bioconjugate Chem* 2003, **14**, 764-773.
42. Ogasawara, S.; Ikeda, A.; Kikuchi, J. *Chem Mater* 2006, **18**, 5982-5987.
43. Waengler, C.; Moldenhauer, G.; Eisenhut, M.; Haberkorn, U.; Mier, W. *Bioconjugate Chemistry* 2008, **19**, 813-820.
44. Plank, C.; Tang, M. X.; Wolfe, A. R.; Szoka, F. C. *Human Gene Therapy* 1999, **10**, 319-332.
45. Tziveleka, L. A.; Psarra, A. M. G.; Tsiourvas, D.; Paleos, C. M. *Journal of Controlled Release* 2007, **117**, 137-146.
46. Okuda, T.; Sugiyama, A.; Niidome, T.; Aoyagi, H. *Biomaterials* 2004, **25**, 537-544.
47. Albert, A.; Goldacre, R.; Phillips, J. *Journal of the Chemical Society* 1948, 2240-2249.
48. Aissaoui, A.; Oudrhiri, N.; Petit, L.; Hauchecorne, M.; Kan, E.; Sainlos, M.; Julia, S.; Navarro, J.; Vigneron, J. P.; Lehn, J. M.; Lehn, P. *Current Drug Targets* 2002, **3**, 1-16.
49. Lee, I.; Athey, B. D.; Wetzel, A. W.; Meixner, W.; Baker, J. R. *Macromolecules* 2002, **35**, 4510-4520.

Table 1. Time-dependency of PAMAM G1/DNA complexation (10:1 N:P ratio).

Incubation time (min)	*% toroids*	*Mean diameter of toroids (nm; mean ± SD)*	*% rods*
10	16	64 ± 10	7
20	32	64 ± 11	10
30	35	69 ± 11	3
45	26	62 ± 9	24
60	25	67 ± 8	30
120	21	79 ± 15	41

Table 2. Time-dependency of 8^{+} Arginine/DNA complexation (10:1 N:P ratio).

Incubation time (min)	*% toroids*	*Mean diameter of toroids (nm; mean ± SD)*	*% rods*
10	27	80 ± 14	0
20	35	68 ± 16	0
30	35	74 ± 13	0
45	27	71 ± 15	0
60	22	76 ± 15	0
120	20	81 ± 13	0

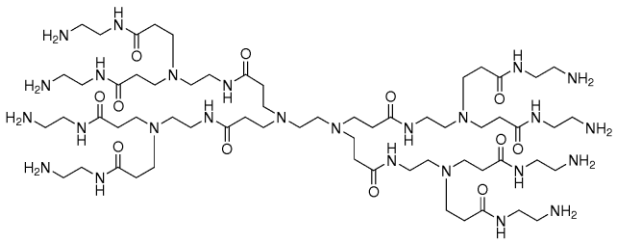

PAMAM G1, **1**

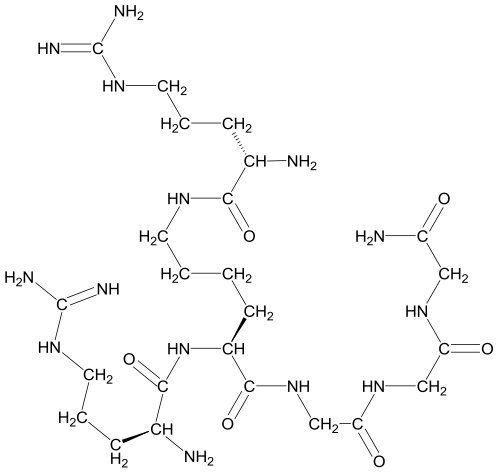

4^+ Arginine, **2**

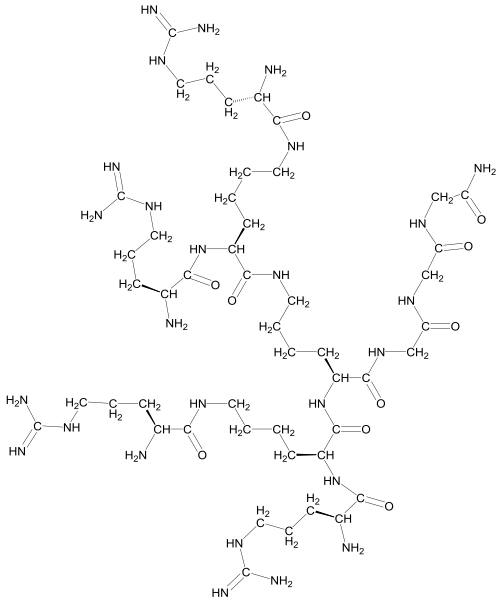

8^+ Arginine, **3**

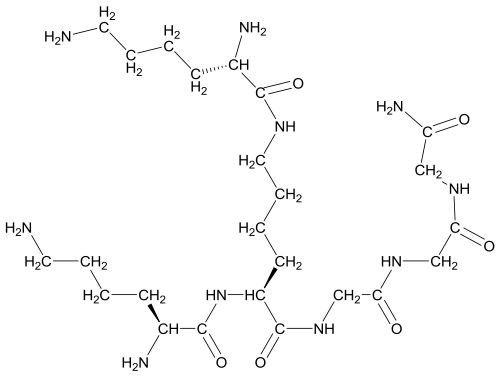

4^+ Lysine, **4**

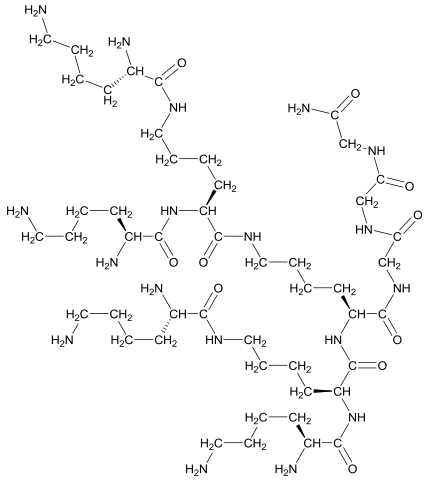

8^+ Lysine, **5**

LEGEND TO FIGURES

Figure. 1. Structure of PAMAM G1**1**, 4^+ Arginine **2**, 8^+ Arginine **3**, 4^+Lysine **4** and 8^+ Lysine **5** dendrimers.

Figure. 2. EtBr assay indicates effective DNA complexation by asymmetric dendrimers. Dendrimers were complexed with DNA in either baxter or autoclaved milli Q water at increasing N:P ratio and equilibrated with EtBr:DNA at a base pair ratio of 1:4. Fluorescence was measured at 485 nm (Ex) and 590 nm (Em) or 544 nm (Ex) and 590 nm (Em) for triplicate samples in each assay and the relative fluorescence intensity calculated. Data from 2-4 separate experiments are shown as mean and SD of triplicate samples at each N:P ratio.

Figure. 3. The difference in morphology of the structures indicates development of toroids at increasing N:P ratio. Dendrimer/DNA complexes were prepared in water (30 min incubation) and visualised by transmission electron microscopy. A - C) PAMAM G1 1:1, 5:1 and 10:1 N:P ratios respectively, D - F) 8^+ Arginine at 1:1, 5:1 and 10:1 N:P ratios respectively. Images are representative of at least 10 sampled fields of view from each of 3 independent experiments carried out at each N:P ratio.

Figure. 4. Dendrimer/DNA complexation is altered by the presence of sodium chloride ions. To determine the role of ions present in solution, PAMAM G1/DNA complexes (A) and 8^+ Arginine asymmetric dendrimer/DNA complexes (B) were prepared in different buffers and DNA complexation tested using the EtBr assay. Data (mean ± SD) are pooled from atleast 2 independent experiments in which samples were tested in triplicate.

Figure. 5. Low generation dendrimers exhibit minimal toxicity. Dendrimer/DNA complexes were prepared in water at defined N:P ratios, incubated for 30 min and then made isotonic by addition of 10 × PBS. Dendrimer/DNA complexes were then incubated with HEK 293T cells and cell viability assessed by propidium iodide staining 24 h later. Data (mean ± SD) are pooled from 3 independent experiments. Controls are untreated cells (control), cells incubated with DNA alone (DNA) or cells treated under identical conditions with DNA/Lipofectamine® complexes (Lipofectamine).

Top of figure

Figure 2

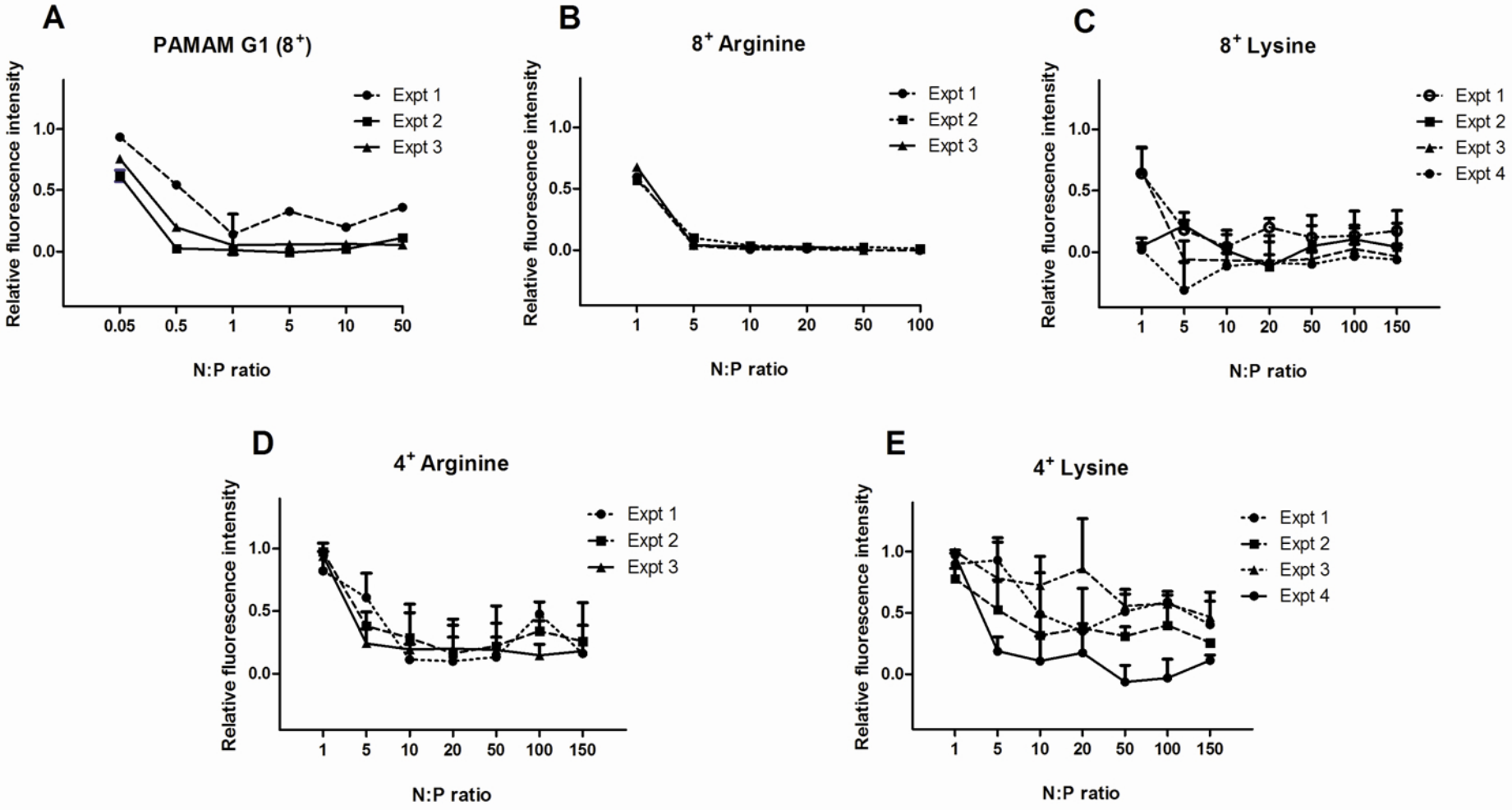

Top of figure

Figure 3

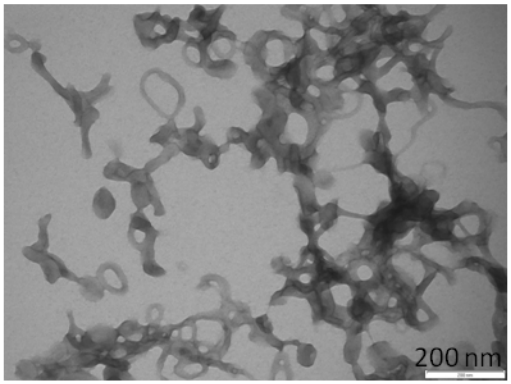

A

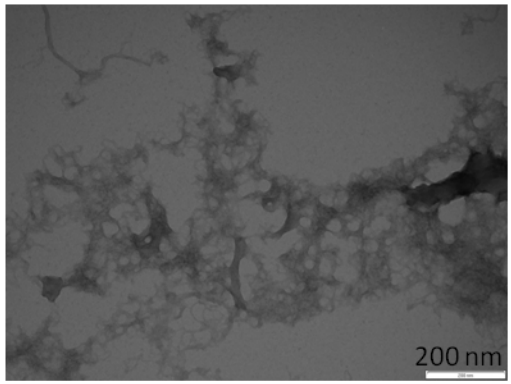

D

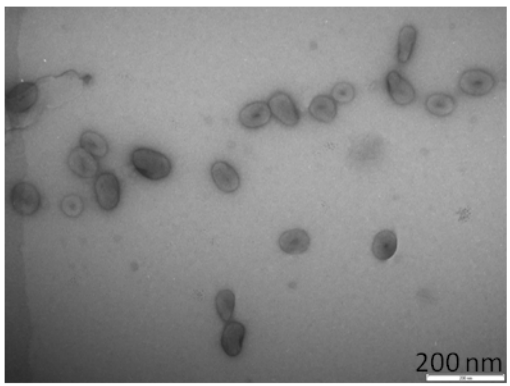

B

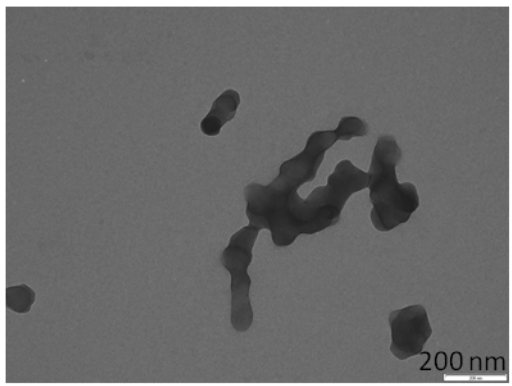

E

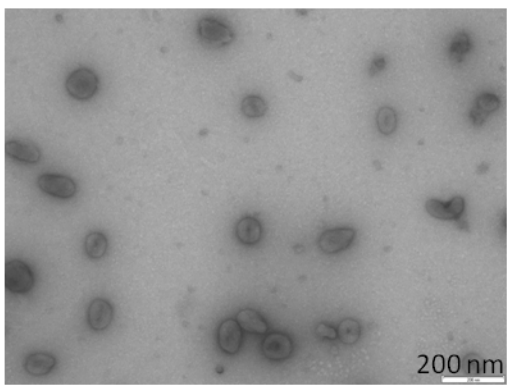

C

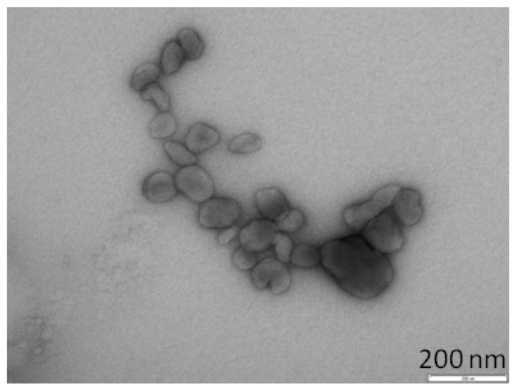

F

Top of figure

Figure 4

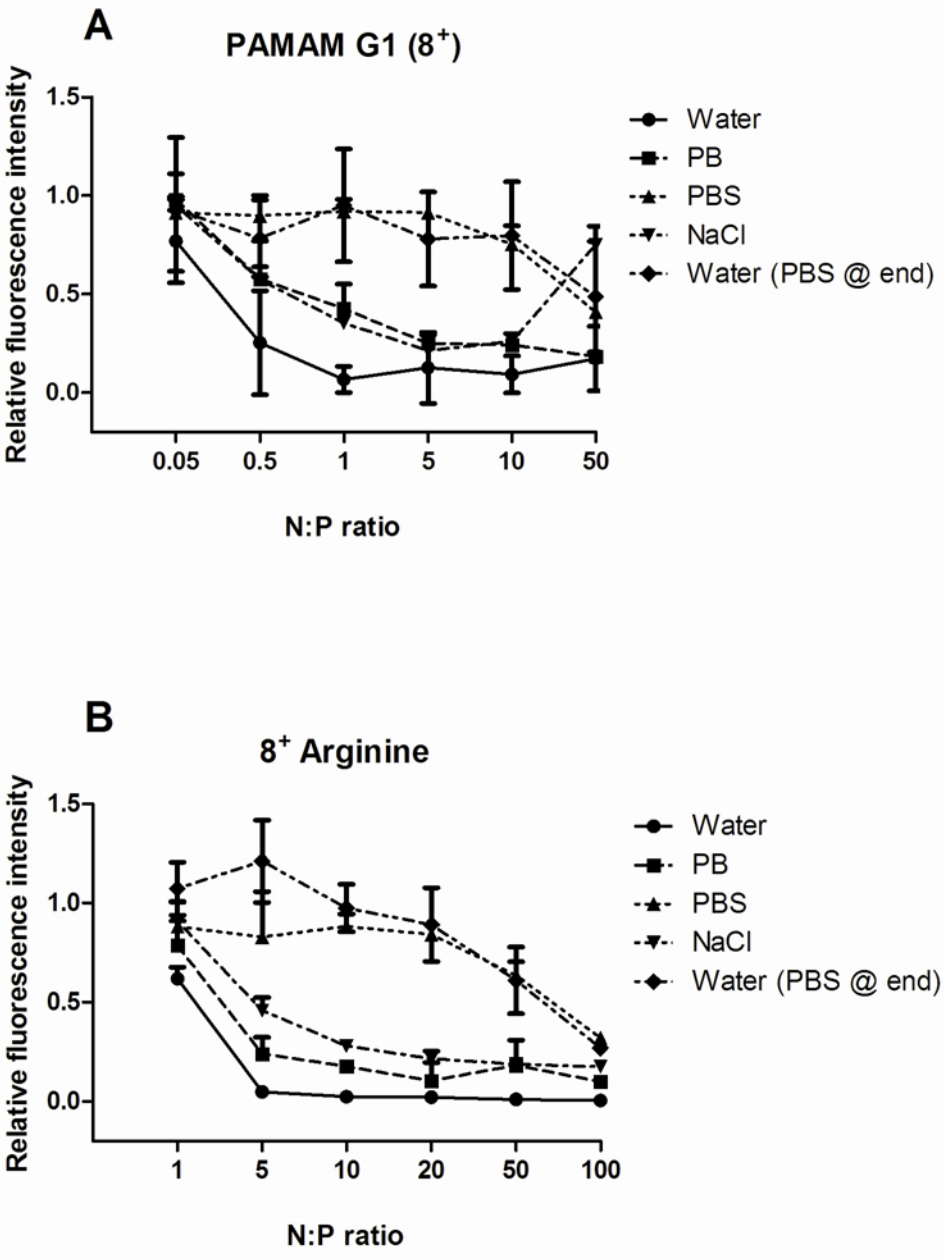

Top of figure

Figure 5